Modelling of Wind Turbines Based on Doubly-Fed Induction Generators for Power System Stability Studies

By
Ram Mohana Vamsee.B (Mtech Student In Electrical Power Systems At Bharati Vidyapeet Deemed University College Of Engineering Pune)(email id- vamsee2703@gmail.com)
Prof. D.S.Bankar (Assistant Professor At Bharati Vidyapeet Deemed University College Of Engineering Pune)

Abstract—This paper deals with modeling of the doubly-fed induction generator (DFIG) and the corresponding converter for stability studies. To enable efficient computation, a reduced-order DFIG model is developed that restricts the calculation to the fundamental frequency component. However, the model enhancement introduced in this paper allows the consideration of the alternating components of the rotor current as well, which is necessary for triggering the crowbar operation. Suitable models are presented for the rotor and grid side converters as well as the dc-link, taking into account all four possible operating modes. The proposed model for speed and pitch angle control can be used when wind and rotor speed variations are significant.

I. INTRODUCTION

THE past decade has seen the emergence of wind as the world's most dynamically growing energy source. In Germany, the installed wind turbine (WT) capacity already surpassed 20GWby the end of the year 2006. In 2020, a total wind power capacity of nearly 50GWis expected, which is more than 50% of the German peak load. In the future, increase of wind power will mainly take place offshore where wind farms with several thousand megawatts connected to the 400-kV grid are expected to be built

With the increasing share of wind in power generation, the dynamic behavior of the power system will change considerably due to different technologies used for wind and conventional generators. Therefore, WTs and wind parks have to be considered in power system dynamic stability studies for which, however, suitable WT models are needed. These models have to compromise between accuracy, for considering relevant dynamic interactions between grid and WT, and simplicity required for the simulation of large systems. WT modeling is a topical research currently conducted by many academic institutions and developers. Different publications came out in the recent past from which, taking into account the aspect of large-scale stability studies, should be mentioned. Despite the effort made, the WT model still needs some refinements, extensions, and adaptations. Based on the experience of the authors working in the development, control, and implementation of a large number of WT up to the 5-MW class, this paper provides a comprehensive report about modelling of WT based on the doubly-fed induction generator (DFIG) for stability kind power system dynamic studies.

Conventional synchronous generators are described for stability analysis by reduced-order models . The same approximation applied to the DFIG results in a similar model , which is applicable with some restrictions. In case of severe grid faults, the DFIG and its associated converter system have to be protected against damage, for which the crowbar (CB) is a

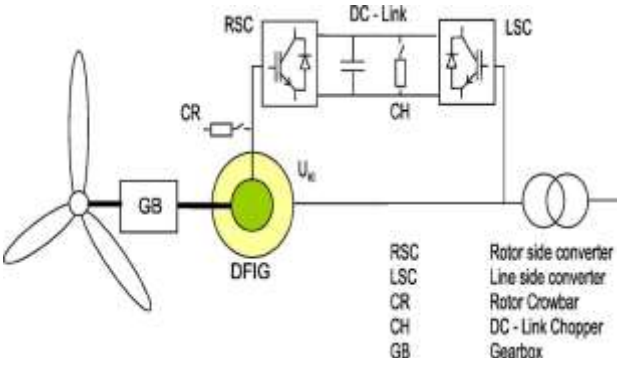

Figure 1 Structure of the DFIG-based wind turbine system.

widely used approach. The CB is a resistance connected to the rotor circuit for a short period for de-energizing the machine while the converter is

disconnected. CB switching is triggered on the basis of rotor current and/or converter dc-link voltage values. However, when the simulation is carried out using a reduced-order model, crucial components for deriving proper triggering signals are left out in both variables. A suitable approach to solve this problem will also be discussed in this paper. In normal operating mode, active and reactive currents and thus P and Q of the DFIG are controlled by the rotor side converter independently. The corresponding controller will be derived based on the DFIG equations. Simplified models are presented also for the converter dc-link and line side converter.

For simulation studies taking wind speed variations into account, or when the rotor shaft speed deviation becomes significant, the turbine's speed and its pitch control systems have to be considered. For this purpose, a generic model is proposed.

II. MODEL OF THE DFIG

A. Detailed Full-Order Model

The DFIG is the most commonly used device for wind power generation. As is generally known, the rotor terminals are fed with a symmetrical three-phase voltage of variable frequency and amplitude. This voltage is supplied by a voltage source converter usually equipped with IGBT-based power electronics circuitry. The basic structure is shown in Fig. 1. The variable frequency rotor voltage permits the adjustment of the rotor speed to match the optimum operating point at any practical wind speed. Protection against over-currents and undesirably high dc voltage is provided by the CB placed on the rotor side. When the rotor current rises and the dc voltage exceeds the upper threshold allowed, the CB thyristor switches are fired and the rotor terminals are short-circuited through the CB resistance.

During this period, the converter control is set to shut down and the DFIG operates as a conventional slip-ring induction machine. Following grid short circuits, the rotor current contains additional alternating components, which correspond with the well-known dc short-circuit currents on the stator side. Alternating rotor currents lead to overshoot of the converter dc-link voltage limit and thus basically influence the CB firing signal derived. For considering the alternating rotor currents in the simulation, a detailed full-order DFIG model is required.

The theoretical background for modeling induction machines are widely developed and are exhaustively dealt with in numerous papers and textbooks. In this paper, the space phasor representation using complex vectors (underlined variables) containing orthogonal direct (d) and quadrature (q) axis components is adopted. Phasors can be represented with respect to different rotating reference frames,and the reference axis may be fixed at any point in the complex plane. The choice of the reference system has a direct bearing on the realization of the desired decoupled control of P and Q. The reference frame for each of the complex variables will be signified using a superscript followed by a sign characterizing the speed of the reference frame and/or a phasor variable indicating that the d-axis chosen corresponds to the direction of the phasor.

Equations (1)–(5) represent the complete set of mathematical relationships that describe the dynamic behaviour of the machine. The per-unit (p.u.) system is adopted as a unit of measurement for all quantities, and the sign convention is chosen in such away that consumed active and inductive reactive powers are positive.

Voltage equations

$$\underline{u}_S^{\angle K} = r_S \underline{i}_S^{\angle K} + \frac{d\underline{\psi}_S^{\angle K}}{dt} + j\omega_K \underline{\psi}_S^{\angle K} \quad (1)$$

$$\underline{u}_R^{\angle K} = r_R \underline{i}_R^{\angle K} + \frac{d\underline{\psi}_R^{\angle K}}{dt} + j(\omega_K - \omega_R)\underline{\psi}_R^{\angle K}. \quad (2)$$

W_k represents an arbitrary speed corresponding to that of the rotating reference frame used denoted by the superscript Lk

.Flux linkages

$$\underline{\psi}_S^{\angle K} = l_S \underline{i}_S^{\angle K} + l_h \underline{i}_R^{\angle K} \quad (3)$$

$$\underline{\psi}_R^{\angle K} = l_h \underline{i}_S^{\angle K} + l_R \underline{i}_R^{\angle K} \quad (4)$$

where $l_S = l_h + l_{\sigma S}$ and $l_R = l_h + l_{\sigma R}$.

Equation of motion:

$$\frac{d\omega_R}{dt} = \frac{1}{\theta_m}\left(\psi_{Sd}^{\angle K} i_{Sq}^{\angle K} - \psi_{Sq}^{\angle K} i_{Sd}^{\angle K} + t_m\right). \quad (5)$$

After some algebraic manipulation, one gets the complex state equation for the stator and rotor circuits as follows:

$$\frac{d\underline{\psi}_S^{\angle K}}{dt} = \left(-\frac{r_s l_R}{l_h(l_{\sigma S}+l_{\sigma R})+l_{\sigma S}l_{\sigma R}} - j\omega_K\right)\underline{\psi}_S^{\angle K} + \frac{l_h r_s}{l_h(l_{\sigma S}+l_{\sigma R})+l_{\sigma S}l_{\sigma R}}\underline{\psi}_R^{\angle K} + \underline{u}_S^{\angle K} \quad (6)$$

$$\frac{d\underline{\psi}_R^{\angle K}}{dt} = \frac{r_R l_h}{l_h(l_{\sigma S}+l_{\sigma R})+l_{\sigma S}l_{\sigma R}}\underline{\psi}_S^{\angle K} - \left(\frac{r_R l_S}{l_h(l_{\sigma S}+l_{\sigma R})+l_{\sigma S}l_{\sigma R}} + j(\omega_k-\omega_R)\right)\underline{\psi}_R^{\angle K} + \underline{u}_R^{\angle K} \quad (7)$$

which, together with the equation of motion (5), form the fullorder model (FOM) that can be used for instantaneous values dynamic time-domain simulations. State variables are the stator and rotor flux components as well as the rotor speed. Often the stator voltage is constant or interpreted as an independent input variable. This allows using the FOM for single-machine infinite-bus investigations. However, in a grid parallel operation, the stator voltage can vary depending on the interaction between DFIG and grid. Basically FOM requires differential equations for the whole network due to the fact that the grid is directly connected to the stator circuit. Using the differential equations of the grid, the stator voltage in (6) can be eliminated. If the FOM is used for time-domain simulation, small integration step sizes are required as a result of the small time constants involved. The small integration time step, in addition to the large number of differential equations especially for the grid, results in considerable simulation efforts when studying large systems.

These disadvantages limit the applicability of the FOM to small grids or even to a single-machine infinite-bus systems.

B. Reduced-Order Model

The reduced-order model (ROM) can then be obtained by neglecting the derivative term in (1), i.e

$$\frac{d\underline{\psi}_S^{\angle \omega_0}}{dt} = 0. \quad (8)$$

This approximation is warranted in the synchronously rotating reference frame only [14]. Accordingly, from this point onward, the synchronously rotating reference frame will be adopted, but the superscript will be abandoned for simplicity of notation. It then follows from (1) for the stator flux linkages that

$$\underline{\psi}_S = \frac{\underline{u}_S - r_S\underline{i}_S}{j\omega_0}. \quad (9)$$

Similarly, another expression for the stator flux linkages can be obtained by eliminating the rotor current in (3) using (4). Thus

$$\underline{\psi}_S = l_S\underline{i}_S + (\underline{\psi}_R - l_h\underline{i}_S)\frac{l_h}{l_R}. \quad (10)$$

From (9) and (10), one gets

$$\underline{u}_S - r_s\underline{i}_S = j\omega_0\left[l_S\underline{i}_S + (\underline{\psi}_R - l_h\underline{i}_S)\frac{l_h}{l_R}\right] \quad (11)$$

which, after rearrangement, results in

$$\underline{u}_S = \underline{z}'\underline{i}_S + \underline{u}' \quad (12)$$

where

$$\underline{z}' = (r_S + j\omega_0 l') \quad (13)$$

$$\underline{u}' = j\omega_0 k_R\underline{\psi}_R \quad (14)$$

are defined as the internal transient impedance and the corresponding transient driving Thévenin voltage source, respectively, with

$$l' = l_s - \frac{l_h^2}{l_R} \quad \text{and} \quad k_R = \frac{l_h}{l_R}.$$

The voltage (12) can be illustrated using the equivalent circuit shown in Fig. 2. The internal voltage in Fig. 2 is a function of the d- and q-components of the rotor flux, which together with the rotor

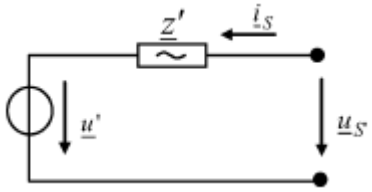

Figure 2 Quasi-stationary equivalent circuit of the DFIM.

speed are state variables of the reduced-order model. The state–space differential equations themselves can be obtained from (2) after eliminating the rotor current using (4). The resulting relationship separated into d- and q-components is

$$\frac{d\psi_{Rd}}{dt} = -\frac{r_R}{l_R}\psi_{Rd} - (\omega_R - \omega_0)\psi_{Rq} + k_R r_R i_{Sd} + u_{Rd} \quad (15)$$

$$\frac{d\psi_{Rq}}{dt} = (\omega_R - \omega_0)\psi_{Rd} - \frac{r_R}{l_R}\psi_{Rq} + k_R r_R i_{Sq} + u_{Rq}. \quad (16)$$

To complete the quasi-stationary model, the equation of motion (5) needs to be modified taking into account the fact that the stator flux is no longer a state variable. This is achieved by eliminating the stator flux first using (3) and then the rotor current using (4), which results in

$$\frac{d\omega_R}{dt} = \frac{1}{\theta_m}\left[k_R(\psi_{Rd} i_{Sq} - \psi_{Rq} i_{Sd}) + t_m\right]. \quad (17)$$

Equations (15)–(17) constitute the quasi-stationary third-order model of the induction machine. The determination of the rotor flux linkages and thus the stator current requires the numerical integration of (15) and (16) and the solution of the algebraic load flow equations of the network into which the machine equivalent circuit (see Fig. 2) is incorporated. The equation of motion (17) has to be solved simultaneously with (15) and (16) to obtain the rotor speed.

C. Enhanced Reduced-Order Model

Since the reduced-order model does not consider the dc-components of the stator current and thus the corresponding alternating rotor currents, it is not suitable for triggering crowbar switching. For this purpose, a model enhancement is proposed in this paper that allows using the ROM further on, but an additional model part is activated when necessary to superimpose the dc-components on the simulation results. The idea is based on the assumption that the stator flux calculated using the ROM is just the slow component of . From (6) follows by considering(8)

$$0 = \left(-\frac{r_s(l_h + l_{\sigma R})}{l_h(l_{\sigma S} + l_{\sigma R}) + l_{\sigma S} l_{\sigma R}} - j\omega_0\right)\underline{\psi}_S^{ROM} + \frac{l_h r_s}{l_h(l_{\sigma S} + l_{\sigma R}) + l_{\sigma S} l_{\sigma R}}\underline{\psi}_R^{ROM} + \underline{u}_S^{ROM} \quad (18)$$

where the superscript “ ”signifies the slow ROM-solution.

In synchronous reference frame, subtracting (18) from (6) results in

$$\frac{d\tilde{\underline{\psi}}_S}{dt} = \left(-\frac{(r_s + r_N)(l_h + l_{\sigma R})}{lh(l_{\sigma S} + l_N + l_{\sigma R}) + (l_{\sigma S} + l_N) l_{\sigma R}} - j\omega_0\right) \cdot \left(\tilde{\underline{\psi}}_S - \underline{\psi}_S^{ROM}\right) \quad (19)$$

under the following assumptions.

1) $\underline{\psi}_R \approx \underline{\psi}_R^{ROM}$, This is nearly fulfilled when the crowbar is switched off. With the presence of the crowbar in the circuit, this assumption is less tenable but still acceptable

2) $\underline{u}_S = \underline{u}_S^{ROM}$ This presupposes that the stator terminal is extended up to the Thevenin equivalent voltage of the grid . In this case, the stator parameters must be also modified as and , where are parameters of equivalent network impedance.

However, it should be emphasized that it is not necessary to know specifically, but the assumption must be, in principle, possible. The corresponding equivalent grid impedance is easily calculated from the well-known shortcircuit capacity . It is obvious that the suggested extension of the stator circuits to a virtual voltage source corresponds with the assumptions used for the standard shortcircuit current calculation. However, the approach presupposes constant equivalent grid impedance. Therefore, the simulation is restricted to cases where the impedance is not significantly affected by the grid fault.

In (19), the stator flux is given as to underscore the approximation used as well as to indicate the extension of the stator to include the grid equivalent circuit. Equation (19) has only as an input variable that is calculated as

$$\underline{\psi}_S^{ROM} = x' \underline{i}_S^{ROM} + k_R \underline{\psi}_R^{ROM} \quad (20)$$

and, as a result, can be solved parallel to the ROM equations.

Besides, the model extension has to proceed in response to grid faults and can be disregarded when the difference between and is negligible. The ROMwith the proposed extension allows the calculation of the rotor currents, including the corresponding

alternating components caused by the dc component of the stator short-circuit currents.

A more detailed description of the proposed model enhancement can be found in . Also comparisons based on simulation results between the full-order model, ROM, and ROM/E are shown in .

III. SPEED AND PITCH CONTROL

The simplified model suggested for power system dynamic studies is shown in Fig. 3. The mechanical power extracted from the wind can be calculated as

$$p_m = \frac{1}{2}\rho A_{rot} C_P(\lambda, \beta) v_w^3 \qquad (21)$$

where

ρ	air density;
A_{rot}	cross-section through which the air mass is streaming;
Cp	power coefficient;
v_W	wind speed.

WT manufacturers give the specific value of for a turbine usually as a function of the pitch-angle and tip-speed ratio

The tip-speed ratio is defined as

$$\lambda = \omega_T R / v_w \qquad (22)$$

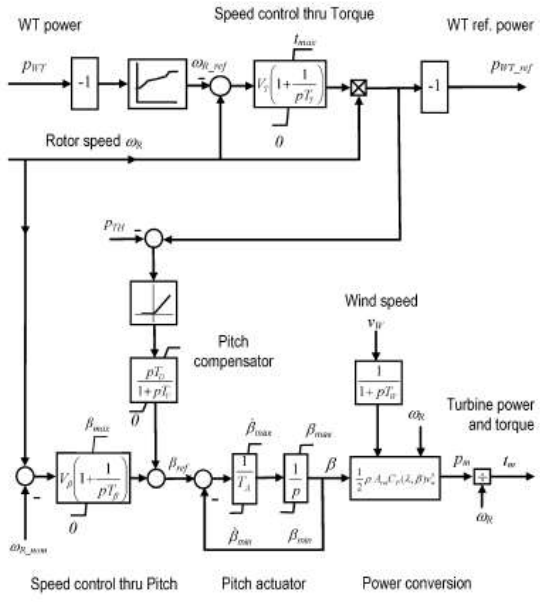

Figure 3 Rotor speed and pitch angle control as well as power conversion model.

where is the radius, and is the speed of the turbine. There is a fixed relationship between and given by the gear transmission ratio. The power calculation according to (21) is based on a single wind speed. However, in reality, the wind speed may differ slightly in direction and intensity across the area traversed by the blades. To consider this effect, the wind speed is supplied through a lag block to the power conversion equation.

The control schema shown in Fig. 3 has two outputs: the WT reference power to be passed on to the converter control and the pitch reference value. Both control channels have speed deviations as input. The torque controller tries to keep the speed at the optimum level corresponding to the actual WT power. The optimum speed is stored in a look-up table. When the speed exceeds the nominal speed, the pitch controller initiates pitching of the blades. Thus, the mechanical power generated by the wind will be reduced and subsequently also the shaft speed. The wind speed is not utilized for control in this schema due to the difficulties with the accuracy of wind speed measurements. Both controllers are permanently active so that switching between different structures is not necessary.

To verify the model, wind ramps from 10 m/s to 14 m/s and back to 10 m/s after further 25 s have been calculated with the simplified model and also with a very detailed model of the manufacturer used for design purposes. The results are shown in Fig. 4. In the range from 10–14 m/s, the nominal power generation and thus the nominal speed are reached. Further increase of the speed must be limited by pitching the rotor blades. This change between the operating modes represents a challenge for the controller applied. As can be seen from the diagrams, the simplified model provides an excellent accuracy from the practical point of view, justifying its use in power system dynamic studies. However, it should be emphasized that this part of the

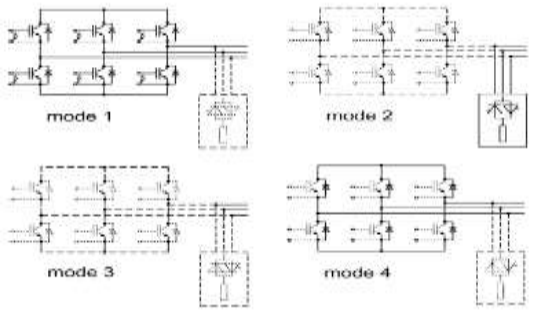

MODEL OF THE CONVERTER

A. Different Operating Modes

To account for the full extent of the interaction between DFIG and the rotor side converter, one has to distinguish between four operating modes (see Fig. 5). The transition logic between the modes is shown in Fig. 6.

Mode 1): Normal mode. Rotor current and rotor voltage are controlled by the IGBTs.

Mode 2): Crowbar mode. Rotor side IGBT-converter switched off, crowbar switched on. When the crowbar is on, the DFIG equations have to be solved with

$$\underline{u}_R = 0$$
$$r_R \rightarrow r_R + r_{\text{Crowbar}}. \qquad (23)$$

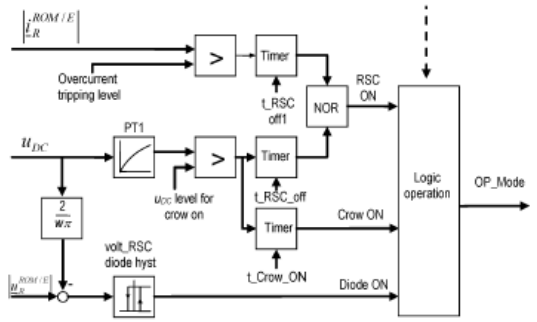

Fig. 6. Switching logic between different operating modes.

The rotor side converter controller is stopped and reset in this mode.

Mode 3): No load mode; rotor side IGBT-converter switched off; rotor-current . In this mode, the rotor flux follows the stator current according to (4) instantaneously, and therefore, does not constitute a state variable when the rotor circuits are open. In fact, based on the assumption , the model described above should be changed considerably for mode 3. However, it is possible to keep the model structure unchanged by using the following approximation:

$$\frac{d\underline{\psi}_R^{ROM}}{dt} = -\frac{1}{T}\left(\underline{\psi}_R^{ROM} - l_h \underline{i}_S^{ROM}\right) \qquad (24)$$

where the fictive time constant must be chosen small enough to guarantee a good approximation of the real undelayed behaviour.

According to our experience, provides already a good approximation. Due to , (19) has to be modified too, as follows.

$$\frac{d\underline{\psi}_S}{dt} = \left(-\frac{r_s + r_N}{l_h + l_{\sigma S} + l_N} - j\omega_0\right) \cdot \left(\underline{\psi}_S - \underline{\psi}_R^{ROM}\right). \qquad (25)$$

The open rotor circuit voltage can be calculated from

$$\underline{u}_R^{ROM/E} = \left(\frac{r_s + r_N}{l_h + l_{\sigma S} + l_N}\left(\underline{\psi}_R^{ROM} - \underline{\psi}_S\right) + j\omega_0 \underline{\psi}_R^{ROM} - j\omega_R \underline{\psi}_S\right) \frac{l_h}{(l_h + l_{\sigma S})}. \qquad (26)$$

Mode 4): Deactivated IGBT-converter mode (rotor side IGBT-converter switched off caused by over-current); generator rotor windings are fed by anti-parallel diodes of rotor side converter. Fast rise of the dc-link voltage is possible. In mode 4, the DFIG can be described by the same equations as used for normal mode. However, the absolute value of rotor voltage is determined by the dc-link voltage only. The phase angle of always corresponds with the phase angle of the rotor current power factor

$$\underline{u}_R = -\frac{2u_{dc}}{w\pi} \cdot e^{j \arg(\underline{i}_R)} \qquad (27)$$

where considers the turns ratio between the reference values of and . To determine whether or not the diode is conducting (refer to Fig. 6), the rotor voltage must be calculated according to (26).

B. Rotor Side Converter

In normal mode, the rotor side converter is used to control the real and reactive power outputs of the machine. Independent control of P and Q can be achieved through rotor current control. As can be seen in (5), the electrical torque keeping balance with the mechanical turbine torque is calculated using the following equation:

$$t_{el} = \psi_{Sd}^{\angle} i_{Sq}^{\angle} - \psi_{Sq}^{\angle} i_{Sd}^{\angle}. \qquad (28)$$

Assuming an orthogonal coordinate system where the real axis always corresponds with the direction of the stator flux, i.e.,

$$\psi_{Sd}^{\angle \psi_S} = \underline{\psi}_S | \qquad (29)$$
$$\psi_{Sq}^{\angle \psi_S} = 0 \qquad (30)$$

follows

$$t_{el} = \underline{\psi}_S |i_{Sq}^{\angle \psi_S}. \quad (31)$$

One can easily deduce that the control of electrical torque can be brought about through the control of the q-axis component of the stator current . Locating the d-axis along the stator flux is a common practice in electrical drives. However, power engineers are more familiar with active and reactive currents. To take account of this preference, d-axis can always be oriented along the stator voltage. It then follows from (9) for the stator flux and voltage

$$\underline{u}_S = r_S \underline{i}_S + j\omega_0 \underline{\psi}_S. \quad (32)$$

Introducing a slightly modified version of the stator voltage

$$\underline{u}_{SR} = \underline{u}_S - r_S \underline{i}_S = j\omega_0 \underline{\psi}_S \quad (33)$$

it is obvious that the stator flux linkage lags behind the stator voltage . Thus, becomes if the direction of is chosen as the d-axis. As a result, the torque equation (28) now becomes

$$t_{el} = |\underline{\psi}_S \, i_{Sd}^{\angle u_{SR}} \quad (34)$$

,

which corresponds with the well-known active current.

Similarly, the imaginary component is equal to the negative of the reactive current. Further simplification is possible by considering the fact that the voltage drop over the stator resistance is always small for the type of large machines employed in WT, viz. . Accordingly, (instead of) will be used as the reference in the subsequent sections. (For a more stringent accuracy requirement, all that is needed is the replacement of by in the corresponding equations.) Control of the DFIG takes place essentially from the rotor side. To calculate the reference values for rotor currents, the steady-state relationship between rotor and stator currents is required.

From (1) and (3) follows (after neglecting the derivative term and setting)

$$\underline{i}_R^{\angle} = -\frac{x_S}{x_h} \underline{i}_S^{\angle} - j\frac{\underline{u}_S^{\angle}}{x_h}. \quad (35)$$

In stator voltage-oriented coordinates

$$i_{Rd}^{\angle u_S} = -\frac{x_S}{x_h} i_{Sd}^{\angle u_S} \quad (36)$$

$$i_{Rq}^{\angle u_S} = -\frac{x_S}{x_h} i_{Sq}^{\angle u_S} - \frac{\underline{u}_S}{x_h}. \quad (37)$$

Assuming that the reference values for active and reactive stator power outputs are known, the corresponding rotor reference currents can be calculated as

$$i_{Rd\_ref}^{\angle u_S} = -\frac{p_{S\_ref}}{|u_S|}\frac{x_S}{x_h} \quad (38)$$

$$i_{Rq\_ref}^{\angle u_S} = \frac{q_{S\_ref}}{|u_S|}\frac{x_S}{x_h} - \frac{\underline{u}_S}{x_h}. \quad (39)$$

The term represents the magnetization current that additionally has to be provided from the rotor side. Fig. 8 shows the control and simulation structure derived from (38) and (39).

Input variables are and , the reference real and reactive power of the wind turbine, respectively. To get the stator reference, the power through LSC is subtracted from these values. is provided by the speed controller, whereas can be chosen arbitrarily within certain limits. The wind turbine references are passed through lag blocks for taking communication delays into account.

C. Line Side Converter

The line or grid side converter has to transmit the active power from the dc-link to the grid so that the dc-link voltage is kept within limits. The corresponding controller and converter model is shown in the upper part of Fig. 10. The output is the active current that is injected into the grid node. Depending on the software used, this current can be converted into an equivalent power. Concerning reactive current generation, the system provides an additional degree of freedom that can be used, e.g., for providing enhanced voltage support to the grid during faults.

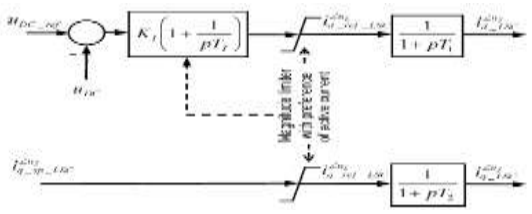

D. Converter DC-Link

A realistic simulation of the crowbar action requires modelling of the converter dc-circuit since the triggering signal is typically derived from the dc-voltage. The dc-circuit contains a capacitor that is charged/discharged by the rotor and grid side converter currents, respectively. However, the capacitor is usually not big enough for smoothing the dc-voltage variations caused by the alternating rotor current. Therefore, accurate rotor currents are the prerequisite for modeling the crowbar switching.

In some applications, the converter dc-link is extended by a chopper to keep the dc-voltage within limits, thereby reducing the number of crowbar actions or even under circumstances forestalling crowbar action altogether.

The time behavior of the converter dc-voltage can be described by the following equation:

$$\frac{du_{dc}}{dt} = \frac{\Delta p_{dc}}{u_{dc} C_{dc}} \tag{46}$$

where

$$\Delta p_{dc} = p_{RSC} + p_{LSC} + p_{Chopper} - p_{RSC\_losses} - p_{LSC\_losses} \tag{47}$$

with

$$p_{RSC} = -(u_{Rd} i_{Rd} + u_{Rq} i_{Rq})$$
$$p_{LSC} = u_{LSC,d} i_{LSC,d} + u_{LSC,q} i_{LSC,q}$$
$$p_{Chopper} = -\frac{u_{dc}^2}{R_{Chopper}} \text{ when chopper on}$$
$$p_{Chopper} = 0 \text{ when chopper off.}$$

The chopper is active when the dc-voltage exceeds a predefined threshold. The converter losses are usually small (approximately 1% of rated output power) and therefore negligible for the desired stability type of simulations. However, for higher accuracy requirements, a polynomial approach can be used for both RSC and LSC.

$$p_{x\_losses} = p_{x0} + a_{x1} |i_x| + a_{x2} i_x^{\,2} \tag{48}$$

where the index stands for RSC or LSC, respectively.

CONCLUSIONS

The simulation of power system dynamics by taking wind farms into account can be carried out using simplified WT models. A reduced-order DFIG model suitable for such simulation studies has been derived in this paper. However, for triggering crowbar switching, more detailed models are necessary, which deliver also the alternating components of the rotor current. For this purpose, a model extension is presented that basically allows the retention of the simplified model and the simulation structure. The rotor side converter control is derived from the DFIG equations. The control schema presented explicitly contains the rotor current so that limitations are easily considered. The line side converter controls the dc-voltage through the active power. The reactive power control channel can be used for providing emergency voltage support during grid faults. Modeling of the speed and pitch control may be necessary when wind fluctuation have to be considered and/or when the WTexperiences large speed deviations.

REFERENCES

[1] I. Erlich and U. Bachmann, “Grid code requirements concerning connection and operation of wind turbines in Germany,” in *Proc. IEEE Power Eng. Soc. General Meeting*, Jun. 12–16, 2005, pp. 2230–2234.

[2] I. Erlich, W.Winter, and A. Dittrich, “Advanced grid requirements for the integration of wind turbines into the German transmission system,” presented at the IEEE Power Eng. Soc. General Meeting, Montreal, QC, Canada, 2006, panel paper 06GM0837

[3] M. A. Pöller, “Doubly-fed induction machine models for stability assessment of wind farms,” presented at the Proc. IEEE PowerTech, Bologna, Italy, Jun. 2003, BPT0-345.

[4] F. M. Hughes, O. Anaya-Lara, N. Jenkins, and G. Strbac, “Control of DFIG-based wind generation for power network support,” *IEEE Trans. Power Syst.*, vol. 20, no. 4, pp. 1958–1966, Nov. 2005.

[5] L. Holdsworth, X. G. Wu, J. B. Ekanayake, and N. Jenkins, “Direct solution method for initializing doubly-fed induction wind turbines in power system dynamic models,” *Proc. Inst. Elect. Eng., Gen., Transm., Distrib.*, vol. 150, no. 3, pp. 334–342, May 2003.

[6] J. B. Ekanayake, L. Holdsworth, X. G. Wu, and N. Jenkins, “Dynamic modelling of doubly fed induction generator wind turbines,” *IEEE*